

This document is the Accepted Manuscript version of a Published Work that appeared in final form in ACS applied materials and interfaces, copyright © American Chemical Society after peer review and technical editing by the publisher. To access the final edited and published work see <http://pubs.acs.org/doi/abs/10.1021/acsami.7b05012>.

Fabrication of Hierarchical Macroporous Biocompatible Scaffolds by Combining Pickering High Internal Phase Emulsion Templates with Three-Dimensional Printing

Ting Yang,¹ Yang Hu,² Chaoyang Wang^{1,*} and Bernard P. Binks^{3,*}

¹ *Research Institute of Materials Science, South China University of Technology, Guangzhou 510640, P.R. China*

² *College of Materials and Energy, South China Agricultural University, Guangzhou 510642, P.R. China*

³ *School of Mathematics and Physical Sciences, University of Hull, Hull HU6 7RX, UK*

Submitted to: ACS Applied Materials & Interfaces

Contains SI

*Corresponding authors: zhywang@scut.edu.cn (CW); b.p.binks@hull.ac.uk (BPB)

Keywords: Pickering; high internal phase emulsions, three-dimensional printing, porous scaffold, poly(L-lactic acid), poly(ε-caprolactone)

This document is the Accepted Manuscript version of a Published Work that appeared in final form in ACS applied materials and interfaces, copyright © American Chemical Society after peer review and technical editing by the publisher. To access the final edited and published work see <http://pubs.acs.org/doi/abs/10.1021/acsami.7b05012>.

Abstract

Biocompatible and biodegradable porous scaffolds with adjustable pore structure have aroused increasing interest in bone tissue engineering. Here, we report a facile method to fabricate hierarchical macroporous biocompatible (HmPB) scaffolds by combining Pickering high internal phase emulsion (HIPE) templates with three-dimensional (3D) printing. HmPB scaffolds composed of a polymer matrix of poly(L-lactic acid), PLLA, and poly(ϵ -caprolactone), PCL, are readily fabricated by solvent evaporation of 3D printed Pickering HIPEs which are stabilized by hydrophobically modified silica nanoparticles (h-SiO₂). The pore structure of HmPB scaffolds is easily tailored to be similar to natural extracellular matrix (ECM) by varying the fabrication conditions of the Pickering emulsion or adjusting the printing parameters. In addition, *in vivo* drug release studies which employ enrofloxacin (ENR) as a model drug indicate the potential of HmPB scaffolds as a drug carrier. Furthermore, *in vivo* cell culture assays prove that HmPB scaffolds possess good biocompatibility as mouse bone mesenchymal stem cells (mBMSCs) can adhere and proliferate well on them. All the results suggest that HmPB scaffolds hold great potential in bone tissue engineering applications.

1. Introduction

Bone tissue engineering provides a promising approach to repair damaged and diseased bones in clinical applications.¹⁻³ In this regard, stem cells are cultured in a three-dimensional porous biocompatible/biodegradable scaffold followed by *in vivo* implantation.⁴⁻⁶ It is highly desirable for the fabricated porous scaffold to mimic the critical characteristics of natural extracellular matrix (ECM), since it serves as an artificial ECM in this approach.^{7,8} Regarding ingredients, materials employed to fabricate scaffolds should be biocompatible and possess an appropriate biodegradability at a rate commensurate with remodeling.⁹⁻¹¹ With respect to structure, an ideal scaffold ought to be highly porous with hierarchical and interconnected pores.¹²⁻¹⁷ A macroporous material (pores of few hundred microns) would maintain the structural stability of the scaffold, promote cell adhesion and proliferation and allow transport of nutrients. Materials with medium sized pores (diameter of tens of microns) would promote vascularization and facilitate the transport of metabolic waste. A material with small pores (diameter of several microns or less) would affect cell behavior such as gene expression.¹⁸ Additionally, adequate mechanical properties to resist physical loads during cell culturing and precisely tailored shape are also required for a desired scaffold.¹⁹⁻²¹ Furthermore, it is noted that local inflammatory response is common in the early days of implantation, and large amounts of antibacterial agents are needed. Hence, the ability to carry and release antibacterial agents efficiently and completely is preferred in the fabrication of scaffolds.^{22,23}

Owing to their brilliant biocompatibility and easy processability, synthetic biodegradable polyesters, especially poly(L-lactic acid), PLLA, and poly(ϵ -caprolactone), PCL, have been extensively used in scaffold fabrication.^{24,25} However, the poor mechanical properties and low bioactivity of pure PCL or PLLA systems has limited their application in the biomedical field. Fortunately, combining PCL, PLLA and bioactive inorganic nanoparticles as fillers inside the

This document is the Accepted Manuscript version of a Published Work that appeared in final form in ACS applied materials and interfaces, copyright © American Chemical Society after peer review and technical editing by the publisher. To access the final edited and published work see <http://pubs.acs.org/doi/abs/10.1021/acsami.7b05012>. polymer matrix provides a promising way to overcome these shortcomings.^{26,27} Among all the facile methods to fabricate highly porous scaffolds with well-defined pore structure, Pickering high internal phase emulsion (HIPE) templates²⁸⁻³¹ and three-dimensional (3D) printing³²⁻³⁵ have aroused attention in recent years. However, a Pickering HIPE, *i.e.* a particle-stabilized emulsion of which the dispersed phase volume fraction is > 0.74 , is only capable of fabricating a material containing medium pores and small pores by solvent evaporation.^{36-39,42,43} Also, 3D printing, a newly emerging method which is based on digital programs and construct the object step by step through dispensing of fluid materials, drew higher demand in the precision of instrumentation and programming to construct refined structure of micron level or below.³² These limitations may be perfectly addressed by combining Pickering HIPE templates with 3D printing. This may also provide a simple way for the preparation of hierarchical porous scaffolds.

According to our previous research, among a variety of bioactive inorganic nanoparticles, PLLA surface-grafted nano-hydroxyapatite (g-HAp) is regarded as the most competent solid particle emulsion stabilizer due to its chemical similarity to natural bone.^{19,43} However, the viscosity of g-HAp-stabilized Pickering emulsions is too low to be printed which constrained its further development. Meanwhile, silica nanoparticles are also widely used as Pickering emulsion stabilizers because of their good biocompatibility and strong mechanical properties.^{47,48} Interestingly, the viscosity of hydrophobically modified silica (h-SiO₂) nanoparticle-stabilized Pickering emulsions is greatly enhanced,⁴⁹ hence providing a promising method to combine Pickering HIPE templates with 3D printing. Sommer *et al.* developed a concentrated oil-in-water Pickering emulsion stabilized by chitosan-modified silica nanoparticles, and then fabricated a hierarchical porous scaffold through 3D printing followed by cross-linking with glutaraldehyde.⁵⁰ However, the above method involves a complex and time-consuming

This document is the Accepted Manuscript version of a Published Work that appeared in final form in ACS applied materials and interfaces, copyright © American Chemical Society after peer review and technical editing by the publisher. To access the final edited and published work see <http://pubs.acs.org/doi/abs/10.1021/acsami.7b05012>. procedure of fabrication and cross-linking, the latter being hard to control. A convenient and effective method is therefore highly desirable in order to obtain hierarchical porous scaffolds.

Herein, we report a facile method to fabricate hierarchical macroporous biocompatible (HmPB) scaffolds by incorporating Pickering HIPE templates into 3D printing for bone tissue engineering. To be specific, we employed h-SiO₂ nanoparticles as the emulsifier to prepare water-in-dichloromethane (W/O) Pickering HIPEs with a polymer matrix of PCL and PLLA. PCL and PLLA are frequently used polymers in biomedical applications. From our exploratory experiments, PCL/h-SiO₂ HmPB scaffolds are too weak for cell adhesion and proliferation, while PLLA/h-SiO₂ HmPB scaffolds possess good anti-compression ability but yield many cracks during drying because of their brittle nature. The as-prepared Pickering HIPEs were printed into cuboid scaffolds with regular macroporous structure. Subsequently, the HmPB scaffolds were readily achieved by solvent evaporation. The preparation conditions in the fabrication of HmPB scaffolds were optimized, and the physical properties such as emulsion morphology, emulsion viscosity and microscopic pore structure were investigated in detail. Finally, drug delivery and release behavior and biocompatibility of HmPB scaffolds were demonstrated.

2. Experimental

2.1. Materials

PCL (weight-average molecular weight $M_w = 80,000 \text{ g mol}^{-1}$) and PLLA with carboxyl end groups ($M_w = 10,000 \text{ g mol}^{-1}$) were purchased from Shandong Medical Instrument Research Institute (Jinan, China). h-SiO₂ nanoparticles (HDK[®] H30 fumed silica possessing 50% SiOH on their surfaces) were obtained from Wacker Chemie (Munich, Germany). Dichloromethane, DCM, was purchased from Guangzhou Chemical Factory (AnalaR, Guangzhou, China). Enrofloxacin (ENR) was bought from Dalian Melone Pharmaceutical Co. Ltd. (Dalian, China). All chemicals were used as received without any further purification. The water used in all experiments was

This document is the Accepted Manuscript version of a Published Work that appeared in final form in ACS applied materials and interfaces, copyright © American Chemical Society after peer review and technical editing by the publisher. To access the final edited and published work see <http://pubs.acs.org/doi/abs/10.1021/acsami.7b05012>. purified by a Millipore purification apparatus whose resistivity was higher than 18 MΩ cm. The

three axis dispensing control system (ADT-TV5300DJ), polypropylene syringe (with a capacity of 30 cm³) and screw dispensing needle (XTLK-18G, with an internal diameter of 0.9 mm) were obtained from Xutong Automatic Technology Co. Ltd. (Shenzhen, China).

2.2. Preparation of W/O Pickering emulsions

h-SiO₂ nanoparticles were chosen as the particulate emulsifier to stabilize W/O HIPEs because of their ability to stabilize Pickering emulsions with viscosity suitable for printing. Firstly, varying volumes of PLLA and PCL were dissolved in 8 mL of DCM. Different amounts of h-SiO₂ nanoparticles were dispersed into the polymer solution with the aid of ultrasound at 0 °C for 10 min. Afterwards, Pickering emulsions were prepared by adding different volumes of water into the oil phase in batches, while applying mechanical shaking after every addition to emulsify the oil-water mixture. The total emulsification time of each sample was kept at 30 min. The obtained Pickering emulsions were coded as P_xS_y-z, where x, y represent the mass/volume of polymer (both PCL and PLLA) and h-SiO₂ in the oil phase and z represents the dispersed phase volume fraction in the emulsion. The detailed experimental formulations are listed in Table 1.

Table 1. Composition of fabricated W/O Pickering emulsions.

Sample	PCL (w/v%)	PLLA (w/v%)	z (vol.%)	h-SiO ₂ (w/v%)	Emulsion stability ^a
P ₆ S _{2.5} -70	3	3	70	2.5	√
P ₆ S _{2.5} -75	3	3	75	2.5	√
P ₆ S _{2.5} -80	3	3	80	2.5	×
P ₆ S _{2.0} -75	3	3	75	2.0	×
P ₆ S _{3.0} -75	3	3	75	3.0	√
P ₇ S _{2.5} -75	3.5	3.5	75	2.5	×
P ₅ S _{2.5} -75	2.5	2.5	75	2.5	√
P ₄ S _{2.5} -75	2	2	75	2.5	√

^a √ represents stable emulsion, × represents unstable emulsion

2.3. Fabrication of hierarchical macroporous biocompatible scaffold

This document is the Accepted Manuscript version of a Published Work that appeared in final form in ACS applied materials and interfaces, copyright © American Chemical Society after peer review and technical editing by the publisher. To access the final edited and published work see <http://pubs.acs.org/doi/abs/10.1021/acsami.7b05012>. HmPB scaffolds were prepared by solvent evaporation from 3D printed W/O Pickering HIPEs. A designed 35x35x7 mm scaffold was fabricated by 3D printing of the as-prepared Pickering HIPEs using an ADT-TV5300DJ three axis dispensing control system. The Pickering HIPE was placed into a 30 cm³ polypropylene syringe (with a piston) and fixed to a screw dispensing needle with an internal diameter of 0.9 mm. Subsequently, the syringe was connected to the dispensing system to obtain the designed structure on a glass substrate at room temperature. For the best result, the pressure was slightly adjusted during the dispensing process for different scaffolds. Finally, after 48 h of solvent evaporation in a fume hood at room temperature, the HmPB scaffold was obtained. The detailed fabrication process is presented in Figure 1.

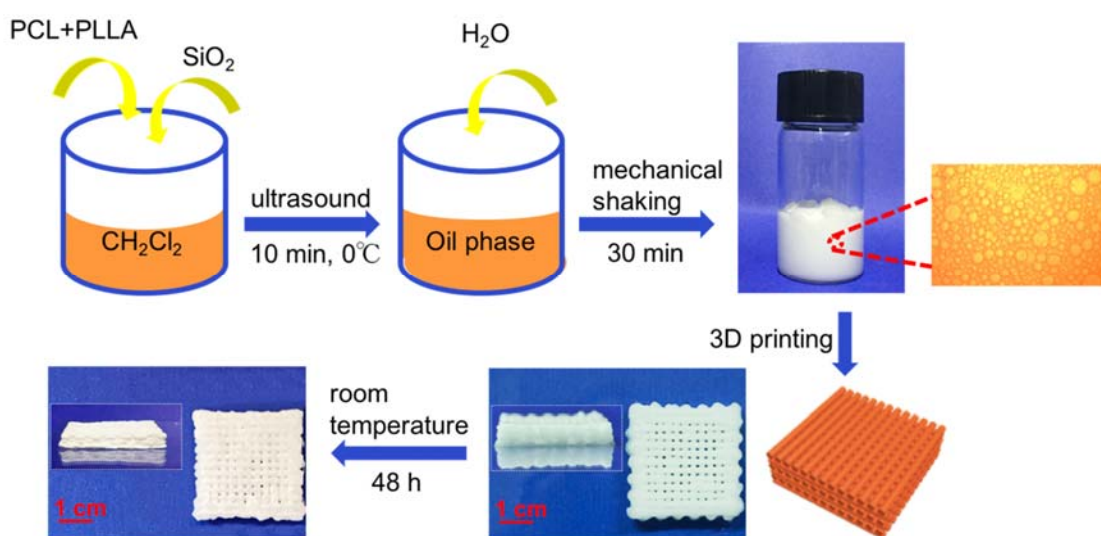


Figure 1. Schematic illustration of the fabrication of a porous scaffold with hierarchical macroporosity.

2.4. Porosity measurement

The porosity (ϵ) of the HmPB scaffold was determined by measuring the apparent density (ρ_s) of the HmPB scaffold and the absolute density (ρ_f), meaning the bulk density of a non-porous nanocomposite film. Values of ρ_s and ρ_f were obtained by calculating the mass/volume ratio of

This document is the Accepted Manuscript version of a Published Work that appeared in final form in ACS applied materials and interfaces, copyright © American Chemical Society after peer review and technical editing by the publisher. To access the final edited and published work see <http://pubs.acs.org/doi/abs/10.1021/acsami.7b05012>. the corresponding scaffolds respectively. Finally, the porosity of the HmPB scaffold was

calculated using

$$\varepsilon (\%) = (1 - \rho_s/\rho_f) \times 100 \quad (1)$$

Three samples from each composition were measured to obtain the average value.

2.5. Rheology

The viscosity of stable Pickering HIPEs was characterized by an ARG-2 rheometer (TA instruments, USA) at 25 °C. Stainless steel parallel plates of diameter 40 mm were employed. The gap between the plates was set at 1 mm. The shear rate was varied from 0.01 s⁻¹ to 10 s⁻¹. To assess the printing performance of stable Pickering HIPEs, oscillatory strain amplitude sweep measurements were conducted. The strain was increased from 0.1% to 300% under a sweep frequency of 1 rad s⁻¹. A low strain (0.1%) was applied immediately after the strain sweep measurement to observe the time-dependent modulus for 200 s, while the angular frequency was kept at 1 rad s⁻¹. All measurements were carried out three times and the average was calculated.

2.6. *In vitro* drug release

The fabrication of ENR-loaded HmPB scaffold is the same as the normal scaffold described above except that 1.2 wt.% of ENR (with respect to the mass of total polymer) was dissolved in DCM before emulsification. The drug release profile of ENR-loaded HmPB scaffold was characterized by measuring the absorbance of ENR at 271 nm using an UV-Vis. spectrophotometer. 20 mg of ENR-loaded HmPB scaffold was immersed into 30 mL phosphate buffer saline (PBS, pH = 7.4) at a constant shaking speed of 100 rpm at 37 °C. At prescribed time intervals, 2 mL of release medium was withdrawn to measure the absorbance. After that, the release medium was added back to the vessels. The release rate was calculated according to the

This document is the Accepted Manuscript version of a Published Work that appeared in final form in ACS applied materials and interfaces, copyright © American Chemical Society after peer review and technical editing by the publisher. To access the final edited and published work see <http://pubs.acs.org/doi/abs/10.1021/acsami.7b05012>. standard absorbance-concentration curve of ENR obtained from known PBS solutions of ENR.

Each formula was measured three times to obtain the average value.

2.7. Characterization

Pickering emulsions were observed by a microscope (Zeiss Axio Lab A1) fitted with a digital camera at 17 °C to reduce the evaporation of DCM. Before observation, all samples were diluted with DCM to enhance the light transmittance. To exam the interior structure of the porous scaffold obtained after air drying of Pickering emulsions and HmPB scaffolds, a Zeiss EVO 18 scanning electron microscope (SEM) with an X-ray energy dispersive spectrometer (EDS) was employed. All samples were frozen by liquid nitrogen and cut by a surgical knife blade to obtain a plate cross section. The obtained sections were observed under an accelerating voltage of 10 kV after being sputter coated with gold.

2.8. *In vitro* cell response

2.8.1. Cell culture

Mouse bone mesenchymal stem cells (mBMSC), purchased from American Type Culture Collection (Manassas), were bred in Dulbecco's Modified Eagle's Medium (DMEM, Gibco) with high glucose. 10% fetal bovine serum (FBS, Gibco) supplemented in DMEM was purchased from Life Technologies (Guangzhou, China). Scaffolds with different composition were sampled into cylinders of diameter 9 mm and height 2 mm. They were then placed into 24-well plates and sanitized with cobalt-60 gamma irradiation for 3 h. 1 mL of mBMSC suspension (1×10^4 cells/well) was seeded onto the samples after it had been pre-treated with culture medium for 12 h. Then these samples were incubated in a humidified incubator with 5% CO₂ at 37 °C.

2.8.2. Cell proliferation

This document is the Accepted Manuscript version of a Published Work that appeared in final form in ACS applied materials and interfaces, copyright © American Chemical Society after peer review and technical editing by the publisher. To access the final edited and published work see <http://pubs.acs.org/doi/abs/10.1021/acsami.7b05012>. To assess the cell proliferation on samples, a cell counting kit-8 (CCK-8, Dojindo Labs, Japan)

was employed. In brief, at each prescribed time point, the culture medium was removed and the CCK-8 working solution was added for incubation for 1 h at 37 °C. Then, the absorbance at 450 nm of the supernatant medium was measured using a Thermo 3001 microplate reader (Thermo, USA).

2.8.3. Cell morphology

Calcein-AM (CCK-8, Dojindo Labs, Japan) was used to observe the cell morphology on samples. In addition, after being cultured for different pre-set times, the cell-seeded samples were rinsed with PBS and then incubated in the standard working solution for 30 min. Subsequently, the samples were washed with PBS again and observed by confocal laser scanning microscopy (CLSM, Leica, Germany).

3. Results and Discussion

3.1. Fabrication of Pickering HIPEs

In this work, hydrophobic silica- stabilized Pickering HIPEs were fabricated from a DCM solution of PLLA and PCL. These particles were chosen as the particle emulsifier because they have the capacity to stabilize Pickering emulsions with appropriate apparent viscosity for 3D printing.⁴⁸ The studied W/O Pickering emulsion formulations are listed in Table 1. Photos of the vessels containing all the emulsions are shown in Figure S1. As shown, stable emulsions cannot be obtained for P₆S_{2.5}-80, P₆S_{2.0}-75 and P₇S_{2.5}-75. With an increase in the internal phase volume fraction or polymer concentration, the difficulty of preparing a stable Pickering emulsion increases due mainly to an increase in the viscosity of the oil phase. The critical viscosity of the oil phase that the emulsification process will be impeded is approximately 92 mPa·S. Decreasing the particulate emulsifier concentration also renders it difficult to make stable emulsions. With

This document is the Accepted Manuscript version of a Published Work that appeared in final form in ACS applied materials and interfaces, copyright © American Chemical Society after peer review and technical editing by the publisher. To access the final edited and published work see <http://pubs.acs.org/doi/abs/10.1021/acsami.7b05012>. fixed internal phase volume fraction ϕ_w , the decreased concentration of stabilizer becomes insufficient to cover the same area of interface, leading to destabilization of formulation P₆S_{2.0}-75. The failure of formulation P₇S_{2.5}-75 was because of the increased viscosity of the oil phase. Emulsions that can be obtained are very stable to coalescence and can be stored over 1 month without any phase separation.

The obtained Pickering emulsions were characterized by optical microscopy. Figure 2 displays the optical microscope images of the samples of different formulation. Most of the droplets are spherical in shape. As observed, when the internal phase volume fraction increased from 70% to 75% (> 74%, the critical point of high internal phase) with the same polymer and particle concentration, the droplets became in close contact from a relatively discrete arrangement. For the same internal phase volume fraction and polymer concentration, increasing the particle concentration from 2.5 wt.% to 3.0 wt.% resulted in a narrow drop size distribution, with the mean diameter decreasing from 20.1 μm to 17.8 μm . By contrast, decreasing the total polymer concentration from 6 wt.% to 4 wt.% resulted in an increase in droplet size (fixed ϕ_w and [particle]). Reduction in the concentration of polymer will result in a decreasing thickness of the polymer film between droplets, thus increasing the difficulty in stabilizing the emulsion. The droplet diameter of nearly 70% of the droplet population in P₆S_{2.5}-75 lies between 10 and 30 μm .

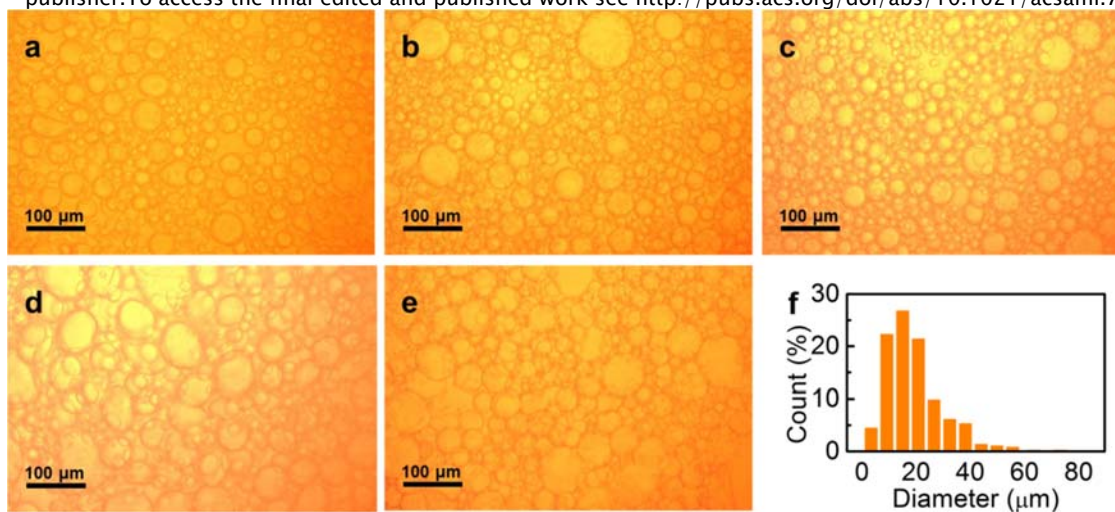
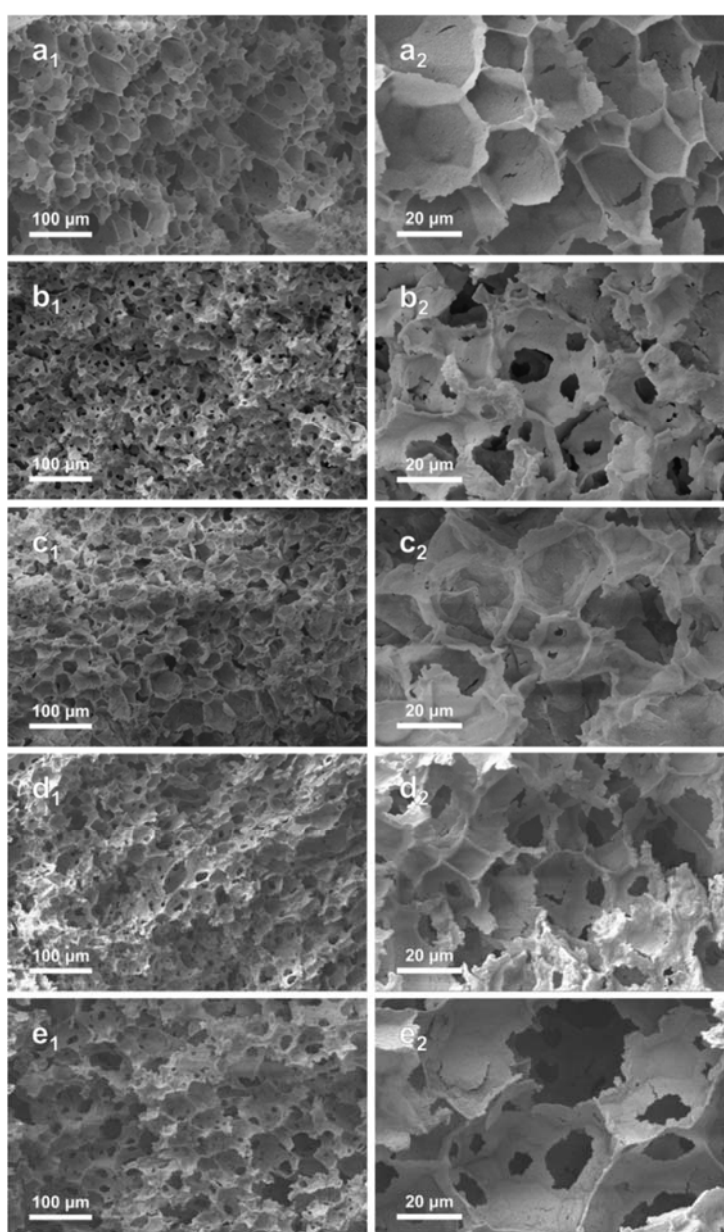


Figure 2. Optical microscope images of stable W/O Pickering emulsions with different formulations: (a) P₆S_{2.5}-70, (b) P₆S_{2.5}-75, (c) P₆S_{3.0}-75, (d) P₅S_{2.5}-75, (e) P₄S_{2.5}-75. (f) Emulsion droplet size distribution of P₆S_{2.5}-75, mean diameter is 20.1 μm.

Subsequently, the internal pore structure of the Pickering emulsion scaffold obtained by natural drying of the emulsions was characterized. After drying at room temperature in a fume hood for 48 h, h-SiO₂ nanoparticles were absorbed onto both PCL and PLLA and the samples were simply transformed into solid scaffolds. Cross sections of these scaffolds were then observed by SEM. The corresponding results are shown in Figure 3. As observed, sample P₆S_{2.5}-70 and P₆S_{3.0}-75 exhibit a closed-cell structure, while sample P₆S_{2.5}-75, P₅S_{2.5}-75 and P₄S_{2.5}-75 possess an open-cell structure, whose pores were interconnected by pore throats. An open-cell structure is an essential property for cells to adhere and proliferate on the scaffold, so only samples P₆S_{2.5}-75, P₅S_{2.5}-75 and P₄S_{2.5}-75 meet the requirement for fabrication of HmPB scaffolds. Owing to the dispersed nature of an emulsion, when ϕ_w was below 74%, the water phase within the droplets was dried separately and uniformly during the evaporation process. The deformation during drying was not enough to break the thick polymer wall between droplets, resulting in a closed-pore structure. On the contrary, due to the close contact of droplets in

This document is the Accepted Manuscript version of a Published Work that appeared in final form in ACS applied materials and interfaces, copyright © American Chemical Society after peer review and technical editing by the publisher. To access the final edited and published work see <http://pubs.acs.org/doi/abs/10.1021/acsami.7b05012>. emulsions whose $\phi_v > 74\%$, the polymer film of their contact area was extremely thin leading to a greater tendency of rupture during solvent evaporation. This results in the formation of throats within the pore walls. Since the polymer films shrink during evaporation, these pores exhibited an irregular shape after drying. In general, the average pore size is similar to that of the precursor emulsion drop diameter.



This document is the Accepted Manuscript version of a Published Work that appeared in final form in ACS applied materials and interfaces, copyright © American Chemical Society after peer review and technical editing by the publisher. To access the final edited and published work see <http://pubs.acs.org/doi/abs/10.1021/acsami.7b05012>.

Figure 3. SEM micrographs of porous scaffolds prepared from stable W/O Pickering emulsions with different formulations: (a₁, a₂) P₆S_{2.5}-70, (b₁, b₂) P₆S_{2.5}-75, (c₁, c₂) P₆S_{3.0}-75, (d₁, d₂) P₅S_{2.5}-75, (e₁, e₂) P₄S_{2.5}-75.

3.2 Fabrication of HmPB scaffolds

The HmPB scaffolds were easily prepared by combining W/O Pickering HIPE templates with 3D printing. Before being printed into HmPB scaffolds, the rheological properties of the Pickering HIPEs which form an open-cell structure were determined. The results displayed in Figure 4(a) indicate that, independent of polymer concentration, all the emulsions present similar rheological behavior. The viscosity decreases progressively with shear rate. The viscosity increases significantly upon increasing the polymer concentration at the same shear rate. We further explored the change of storage modulus (G') and loss modulus (G'') of emulsion P₆S_{2.5}-75 as a function of strain and time. As shown in Figure 4(b), when applying a strain below 80% to this emulsion, G' remains greater than G'' and the emulsion presents a solid-like state. Above 80% strain however, G' decreases becoming less than G'' and the emulsion began to present a liquid-like state. When the strain reached 250%, it was reduced to the initial strain of 0.01% and the emulsion returned to a solid-like state immediately, similar to that of printable ceramic emulsions reported recently.^{40,41} The viscosity results suggest that the Pickering HIPEs are printable, and can maintain their structure once printed without significant deformation.

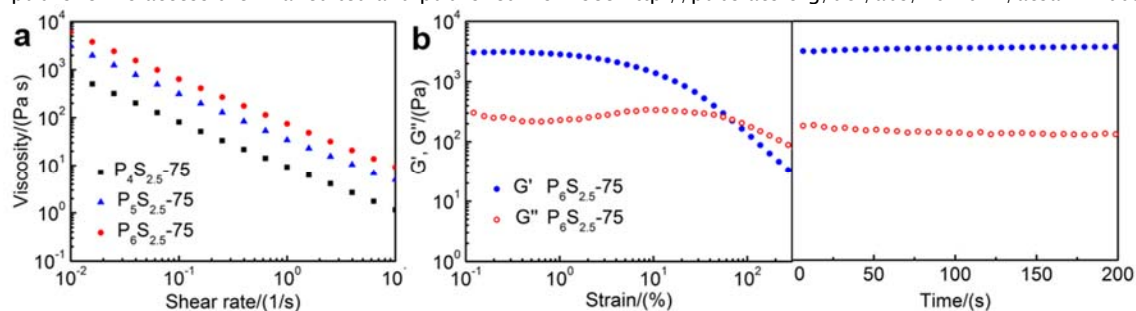


Figure 4. (a) Curves of viscosity *versus* shear rate for W/O Pickering HIPEs which lead to interconnected open-cell structure. (b) Strain-sweep profile for scaffold P₆S_{2.5}-75 (left) and G' , G'' as a function of time at a strain of 0.1% (right).

Once the competent Pickering HIPEs were printed into the pre-designed structure and dried completely, HmPB scaffolds were finally obtained. The key parameter for successful printing was the magnitude of the pressure applied to the syringe. The optimum value however (between 0.1 and 0.2 MPa) is dependent on the viscosity of the emulsion. Subsequently, the internal pore structure of the HmPB scaffolds was characterized and some images are shown in Figure S2. Meanwhile, SEM micrographs of the surface of the printed lines are presented in Figure S3. A photo of such a HmPB scaffold is shown in Figure S4. As seen in Figure S4, HmPB scaffolds possess interconnected regular macropores which are obtained by 3D printing. As SEM images of HmPB scaffolds show, the scaffolds possess medium-sized pores and small pores which are connected by ruptures on pore walls. Thus, by combining W/O Pickering HIPE templates with 3D printing, the HmPB scaffolds were endowed with an interconnected hierarchical macroporous structure, which included macropores, medium-sized pores and small pores. While the large macropores originated *via* 3D printing, the medium-sized pores and small pores originated during solvent evaporation. As one important characteristic of biocompatible scaffolds, the porosities of the HmPB scaffolds were measured too. The values are given in Table 2. The porosities of the HmPB scaffolds are all higher than 98%, much higher than conventional

This document is the Accepted Manuscript version of a Published Work that appeared in final form in ACS applied materials and interfaces, copyright © American Chemical Society after peer review and technical editing by the publisher. To access the final edited and published work see <http://pubs.acs.org/doi/abs/10.1021/acsami.7b05012>. Pickering HIPE scaffolds with similar dispersed phase volume fraction (typically < 90%).^{31,42-45}

Owing to the high porosity and the hierarchical macroporous structure, the HmPB scaffolds can mimic the architecture of the native ECM. We hypothesized that the structure of HmPB scaffolds enabled them to be well suited for cell adhesion, proliferation, migration and differentiation.

Table 2. Physical properties of HmPB scaffolds.

Sample	Absolute density (g cm ⁻³)	Apparent density (g cm ⁻³)	Porosity (%)
P6S2.5-75	2.303	0.045	98.0
P5S2.5-75	2.297	0.040	98.3
P4S2.5-75	2.290	0.038	98.3

3.3. *In vitro* drug delivery characterization

The implantation of foreign scaffolds into the body may cause serious inflammation especially in the initial period such that large quantities of anti-inflammatory agents are needed. The performance of HmPB scaffolds as a drug carrier was explored. In this work, enrofloxacin (ENR) was chosen as the model medicine. As ENR possesses a wide anti-bacterial spectrum, strong bactericidal activity and low toxicity, it is thus widely applied in veterinary clinics. After ENR-loaded HmPB scaffolds were fabricated by the same method as normal scaffolds except that ENR was dissolved in DCM before emulsification, the drug release profile was measured using UV spectrophotometry. The results are shown in Figure 6. As observed, enrofloxacin released nearly 80% in the first 2.5 h, and the release rate of all samples reached over 98% after 10 h. Hence, the HmPB scaffolds provide both a rapid and complete drug release profile.

We also employed Sudan red (coloring the scaffolds orange) to visualize the drug loaded on HmPB scaffolds after dissolving it in DCM before emulsification. As the insets in Figure 6 show, a composite structure can be obtained employing a regular Pickering HIPE and a second

This document is the Accepted Manuscript version of a Published Work that appeared in final form in ACS applied materials and interfaces, copyright © American Chemical Society after peer review and technical editing by the publisher. To access the final edited and published work see <http://pubs.acs.org/doi/abs/10.1021/acsami.7b05012>. Pickering HIPE containing Sudan as an exemplary drug. The regular Pickering HIPE is used in the bottom half of the structure, whereas the ‘drug-loaded’ Pickering HIPE is positioned in the top (top image) or in the middle of the scaffold (bottom image). In other words, we can load the drugs or several other sensitive constituents like proteins on any concrete position in HmPB scaffolds to endow them with multi-functionality. Also, scaffolds with different structure can be obtained by switching the printing procedure. Thus, the functional and structural designability of HmPB scaffolds were improved markedly and their development in bone tissue engineering was further promoted.

To determine the release mechanisms, three different kinetic models (First-order model, Higuchi model and Hixson–Crowell model) were employed to fit the release profiles of ENR from the ENR-loaded HmPB scaffolds. Equation of each model are presented in Support Information, and the values of correlation coefficient (R^2) are listed in Table S1. Model with larger value of R^2 was supposed to be the more appropriate model for the release profiles. As shown in Table S1, the values of R^2 obtained from the linear fitting of Hixson–Crowell model were the biggest of all the models. Therefore, Hixson–Crowell model can better fit the release profiles of ENR from the ENR-loaded HmPB scaffolds. And the release of ENR from the scaffolds is based on drug erosion from carriers.

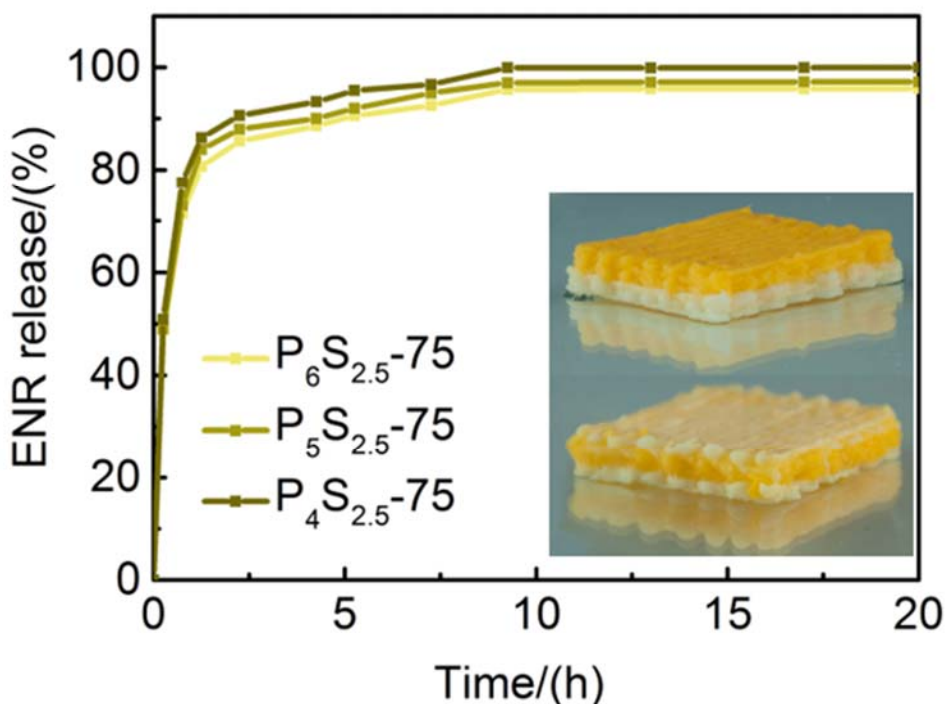


Figure 5. *In vitro* release profile of ENR from ENR-loaded HmPB scaffolds incubated in PBS at 37 °C. Inset photos show HmPB scaffolds of P₆S_{2.5}-75 with loaded ENR in different positions visualized by Sudan.

3.4. *In vitro* biocompatibility assessment

To assess the biocompatibility of as-prepared HmPB scaffolds, *in vitro* cell culture experiments were carried out on formulation P₆S_{2.5}-75. Herein, mBMSCs were seeded onto the HmPB scaffolds *in vitro*. An CCK-8 assay was employed to evaluate the viability of mBMSCs on samples after a different number of days culture. The viability of mBMSCs shown in Figure 7 indicates that mBMSCs can adhere and proliferate on HmPB scaffolds. As observed, viable mBMSCs on HmPB scaffolds proliferated significantly over the incubation period. The viability of mBMSCs on HmPB scaffolds is significantly higher than on porous scaffolds fabricated by Pickering HIPE templates only.⁴³ The excellent biocompatibility of the ingredients of HmPB

This document is the Accepted Manuscript version of a Published Work that appeared in final form in ACS applied materials and interfaces, copyright © American Chemical Society after peer review and technical editing by the publisher. To access the final edited and published work see <http://pubs.acs.org/doi/abs/10.1021/acsami.7b05012>. scaffolds is friendly for cell culturing. Also, HmPB scaffolds possess millimeter-sized macropores which are absent in traditional Pickering emulsion scaffolds.^{31,42,43} This renders the structure of HmPB scaffolds to be more similar to that of ECM, promoting cell adhesion and proliferation.

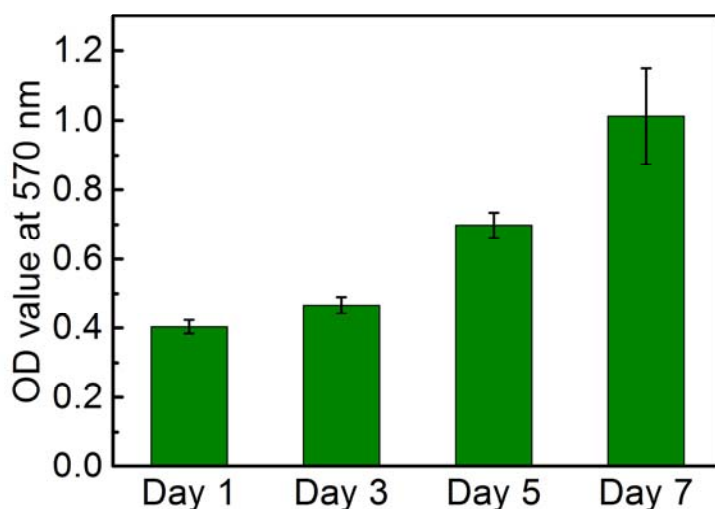


Figure 6. Cell viability of mBMSCs after 1, 3, 5 and 7 days of culture on HmPB scaffold P₆S_{2.5-75} measured by CCK-8 assay. OD stands for optical density, the result of CCK-8 assay.

For further assessment of the biocompatibility of the HmPB scaffolds, the morphology of mBMSCs was characterized using confocal laser scanning microscopy. Representative images of mBMSCs on scaffold P₆S_{2.5-75} after 3, 5 and 7 days of culture are shown in Figure 8. As observed, the mBMSCs adhered and spread well along the surface of the sample after 3 days of culture, and exhibited ellipsoidal morphology with slight collapse in the center. After 5 days of culture, the mBMSCs started to change into elongated pseudopodia. Moreover, after 7 days of culture, the mBMSCs spread completely and uniformly on the surface of the scaffold forming a confluent layer, indicating outstanding cell viability. Combining with the cell viability from

This document is the Accepted Manuscript version of a Published Work that appeared in final form in ACS applied materials and interfaces, copyright © American Chemical Society after peer review and technical editing by the publisher. To access the final edited and published work see <http://pubs.acs.org/doi/abs/10.1021/acsami.7b05012>. CCK-8 assay, it can be concluded that HmPB scaffolds are equipped with good biocompatibility

with mBMSCs. Hence, the obtained HmPB scaffolds possess great promise to induce cell growth in the biomedical field.

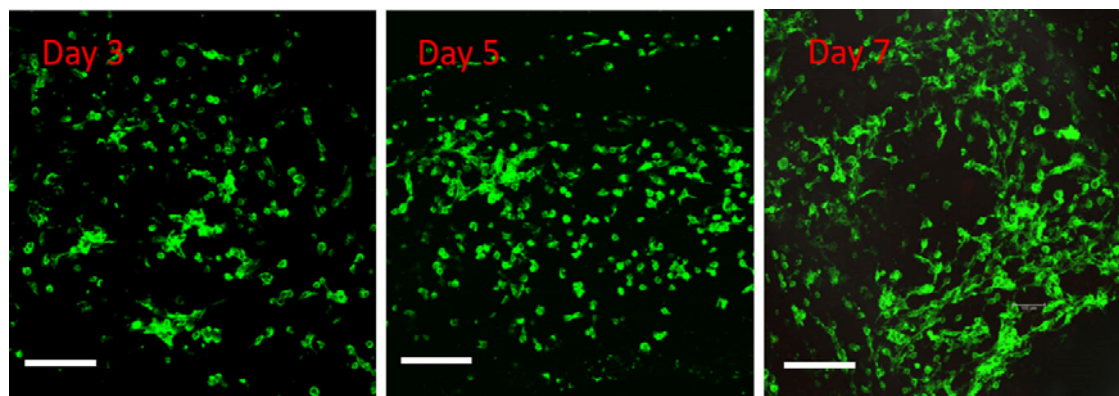


Figure 7. Confocal laser scanning microscope images of mBMSCs seeded on scaffold P₆S_{2.5-75} after 3, 5 and 7 days culture. Scale bars are 200 μm .

4. Conclusions

HmPB scaffolds with hierarchical (including macropores, medium pores and small pores) and interconnected pore structures were simply fabricated by combining Pickering HIPE templates with 3D printing. More specifically, HmPB scaffolds of a polymer matrix of PLLA and PCL are readily fabricated by solvent evaporation of 3D printed Pickering HIPEs stabilized by h-SiO₂ nanoparticles. The fabrication conditions were optimized by adjusting the polymer and particle concentrations and the water droplet volume fraction. The pore structure of as-prepared HmPB scaffolds is tailored to be similar to that of natural extracellular matrix (ECM) by varying the fabricating conditions of the Pickering emulsions or adjusting the printing parameters. The anti-inflammatory drug ENR was loaded into HmPB scaffolds easily and efficiently. *In vivo* drug

This document is the Accepted Manuscript version of a Published Work that appeared in final form in ACS applied materials and interfaces, copyright © American Chemical Society after peer review and technical editing by the publisher. To access the final edited and published work see <http://pubs.acs.org/doi/abs/10.1021/acsami.7b05012>. release profile studies indicate that HmPB scaffolds can be used as drug carrier and meet the demand of anti-inflammation in the early period of implantation. *In vivo* cell culture assays proved that the obtained HmPB scaffolds can support the adhesion and proliferation of mBMSCs on them, which indicate the excellent biocompatibility of HmPB scaffolds. All the above results demonstrate a great potential for bone tissue engineering application of the as-prepared HmPB scaffolds.

ASSOCIATED CONTENT

Supporting Information.

The following files are available free of charge.

Digital photos of and SEM micrographs of emulsions and scaffolds (PDF)

AUTHOR INFORMATION

Corresponding Authors

zhywang@scut.edu.cn (CW); b.p.binks@hull.ac.uk (BPB).

Author Contributions

The manuscript was written through contributions of all authors. All authors have given approval to the final version of the manuscript.

Funding Sources

National Natural Science Foundation of China (21474032)

Natural Science Foundation of Guangdong Province (2016A030310461)

This document is the Accepted Manuscript version of a Published Work that appeared in final form in ACS applied materials and interfaces, copyright © American Chemical Society after peer review and technical editing by the publisher. To access the final edited and published work see <http://pubs.acs.org/doi/abs/10.1021/acsami.7b05012>.

ACKNOWLEDGMENT

This work was financially supported by National Natural Science Foundation of China (21474032) and Natural Science Foundation of Guangdong Province (2016A030310461).

ABBREVIATIONS

HmPB, hierarchical macroporous biocompatible scaffolds; HIPE, high internal phase emulsion; 3D, three-dimensional; ECM, extracellular matrix; PLLA, poly(L-lactic acid); PCL, poly(ϵ -caprolactone); h-SiO₂, hydrophobically modified silica nanoparticles; mBMSCs, mouse bone mesenchymal stem cells; g-HAp, PLLA surface-grafted nano-hydroxyapatite; W/O, water-in-oil; ENR, enrofloxacin; DCM, dichloromethane; G', storage modulus; G'', loss modulus.

This document is the Accepted Manuscript version of a Published Work that appeared in final form in ACS applied materials and interfaces, copyright © American Chemical Society after peer review and technical editing by the publisher. To access the final edited and published work see <http://pubs.acs.org/doi/abs/10.1021/acsami.7b05012>.

References

- [1] Won, J.-E.; Yun, Y.-R.; Jang, J.-H.; Yang, S.-H.; Kim, J.-H.; Chrzanowski, W.; Wall, I. B.; Knowles, J. C.; Kim, H.-W. Multifunctional and Stable Bone Mimic Proteinaceous Matrix for Bone Tissue Engineering. *Biomaterials* **2015**, *56* 46-57.
- [2] Liu, H.; Peng, H.; Wu, Y.; Zhang, C.; Cai, Y.; Xu, G.; Li, Q.; Chen, X.; Ji, J.; Zhang, Y.; OuYang, H.W. The Promotion of Bone Regeneration by Nanofibrous Hydroxyapatite/Chitosan Scaffolds by Effects on Integrin-Bmp/Smad Signaling Pathway in Bmscs. *Biomaterials* **2013**, *18*, 4404-4417.
- [3] Xu, Z.-L.; Lei, Y.; Yin, W.-J.; Chen, Y.-X.; Ke, Q.-F.; Guo, Y.-P.; Zhang, C.-Q. Enhanced Antibacterial Activity and Osteoinductivity of Ag-Loaded Strontium Hydroxyapatite/Chitosan Porous Scaffolds for Bone Tissue Engineering. *J. Mater. Chem. B* **2016**, *48*, 7919-7928.
- [4] Martinez Avila, H.; Feldmann, E.-M.; Pleumeekers, M. M.; Nimeskern, L.; Kuo, W.; de Jong, W. C.; Schwarz, S.; Muller, R.; Hendriks, J.; Rotter, N.; van Osch, G. J. V. M.; Stok, K.; S. Gatenholm, P. Novel Bilayer Bacterial Nanocellulose Scaffold Supports Neocartilage Formation in Vitro and in Vivo. *Biomaterials* **2015**, *44*, 122-133.
- [5] Cui, Y.; Liu, Y.; Cui, Y.; Jing, X.; Zhang, P.; Chen, X. The Nanocomposite Scaffold of Poly(Lactide-Co-Glycolide) and Hydroxyapatite Surface-Grafted with L-Lactic Acid Oligomer for Bone Repair. *Acta Biomater.* **2009**, *7*, 2680-2692.
- [6] Geesala, R.; Bar, N.; Dhoke, N. R.; Basak, P.; Das, A. Porous Polymer Scaffold for on-Site Delivery of Stem Cells - Protects from Oxidative Stress and Potentiates Wound Tissue Repair. *Biomaterials* **2016**, *159*, 1-13.
- [7] Xu, Z.-L.; Lei, Y.; Yin, W.-J.; Chen, Y.-X.; Ke, Q.-F.; Guo, Y.-P.; Zhang, C.-Q. Enhanced Antibacterial Activity and Osteoinductivity of Ag-Loaded Strontium Hydroxyapatite/Chitosan

This document is the Accepted Manuscript version of a Published Work that appeared in final form in ACS applied materials and interfaces, copyright © American Chemical Society after peer review and technical editing by the publisher. To access the final edited and published work see <http://pubs.acs.org/doi/abs/10.1021/acsami.7b05012>. Porous Scaffolds for Bone Tissue Engineering. *J. Mater. Chem. B* **2016**, *48*, 7919-7928.

[8] Yu, X.; Qian, G.; Chen, S.; Xu, D.; Zhao, X.; Du, C. A Tracheal Scaffold of Gelatin-Chondroitin Sulfate-Hyaluronan-Polyvinyl Alcohol with Orientated Porous Structure. *Carbohydr. Polym.* **2017**, *159*, 20-28.

[9] Chen, K.-Y.; Liao, W.-J.; Kuo, S.-M.; Tsai, F.-J.; Chen, Y.-S.; Huang, C.-Y.; Yao, C.-H. Asymmetric Chitosan Membrane Containing Collagen I Nanospheres for Skin Tissue Engineering. *Biomacromolecules* **2009**, *6*, 1642-1649.

[10] Beavers, K. R.; Werfel, T. A.; Shen, T.; Kavanaugh, T. E.; Kilchrist, K. V.; Mares, J. W.; Fain, J. S.; Wiese, C. B.; Vickers, K. C.; Weiss, S. M.; Duvall, C. L. Porous Silicon and Polymer Nanocomposites for Delivery of Peptide Nucleic Acids as Anti-Microrna Therapies. *Adv. Mater.* **2016**, *36*, 7984-7992.

[11] Hong, J. K.; Madhally, S. V. Three-Dimensional Scaffold of Electrospayed Fibers with Large Pore Size for Tissue Regeneration. *Acta Biomater.* **2010**, *12*, 4734-4742.

[12] Zhang, S.; Jiang, Z.; Shi, J.; Wang, X.; Han, P.; Qian, W. An Efficient, Recyclable, and Stable Immobilized Biocatalyst Based on Bioinspired Microcapsules-in-Hydrogel Scaffolds. *ACS Appl. Mater. Interfaces* **2016**, *38*, 25152-25161.

[13] Zhang, Y.; Xia, L.; Zhai, D.; Shi, M.; Luo, Y.; Feng, C.; Fang, B.; Yin, J.; Chang, J.; Wu, C. Mesoporous Bioactive Glass Nanolayer-Functionalized 3d-Printed Scaffolds for Accelerating Osteogenesis and Angiogenesis. *Nanoscale* **2015**, *45*, 19207-19221.

[14] Yang, Y.; Wang, H.; Yan, F.-Y.; Qi, Y.; Lai, Y.-K.; Zeng, D.-M.; Chen, G.; Zhang, K.-Q. Bioinspired Porous Octacalcium Phosphate/Silk Fibroin Composite Coating Materials Prepared by Electrochemical Deposition. *ACS Appl. Mater. Interfaces* **2015**, *10*, 5634-5642.

[15] Castro, N. J.; O'Brien, J.; Zhang, L. G. Integrating Biologically Inspired Nanomaterials and

This document is the Accepted Manuscript version of a Published Work that appeared in final form in ACS applied materials and interfaces, copyright © American Chemical Society after peer review and technical editing by the publisher. To access the final edited and published work see <http://pubs.acs.org/doi/abs/10.1021/acsami.7b05012>.

Table-Top Stereolithography for 3d Printed Biomimetic Osteochondral Scaffolds. *Nanoscale* **2015**, *33*, 14010-14022.

[16] Xie, C.; Lu, X.; Han, L.; Xu, J.; Wang, Z.; Jiang, L.; Wang, K.; Zhang, H.; Ren, F.; Tang, Y. Biomimetic Mineralized Hierarchical Graphene Oxide/Chitosan Scaffolds with Adsorbability for Immobilization of Nanoparticles for Biomedical Applications. *ACS Appl. Mater. Interfaces* **2016**, *3*, 1707-1717.

[17] Khapli, S.; Rianasari, I.; Blanton, T.; Weston, J.; Gilardetti, R.; Neiva, R.; Tovar, N.; Coelho, P. G.; Jagannathan, R. Fabrication of Hierarchically Porous Materials and Nanowires through Coffee Ring Effect. *ACS Appl. Mater. Interfaces* **2014**, *23*, 20643-20653.

[18] Xu, T.; Miszuk, J. M.; Zhao, Y.; Sun, H.; Fong, H. Electrospun Polycaprolactone 3d Nanofibrous Scaffold with Interconnected and Hierarchically Structured Pores for Bone Tissue Engineering. *Adv. Healthcare Mater.* **2015**, *15*, 2238-2246.

[19] Donius, A. E.; Liu, A.; Berglund, L. A.; Wegst, U. G. K. Superior Mechanical Performance of Highly Porous, Anisotropic Nanocellulose-Montmorillonite Aerogels Prepared by Freeze Casting. *J. Mech. Behav. Biomed. Mater.* **2014**, *37*, 88-99.

[20] Zhang, P.; Hong, Z.; Yu, T.; Chen, X.; Jing, X. In Vivo Mineralization and Osteogenesis of Nanocomposite Scaffold of Poly (Lactide-Co-Glycolide) and Hydroxyapatite Surface-Grafted with Poly(L-Lactide). *Biomaterials* **2009**, *1*, 58-70.

[21] Dashnyam, K.; Perez, R. A.; Singh, R. K.; Lee, E.-J.; Kim, H.-W. Hybrid Magnetic Scaffolds of Gelatin-Siloxane Incorporated with Magnetite Nanoparticles Effective for Bone Tissue Engineering. *RSC Adv.* **2014**, *77*, 40841-40851.

[22] Cezar, C. A.; Kennedy, S. M.; Mehta, M.; Weaver, J. C.; Gu, L.; Vandeburgh, H.; Mooney, D. J. Biphasic Ferrogels for Triggered Drug and Cell Delivery. *Adv. Healthcare Mater.* **2014**, *11*,

This document is the Accepted Manuscript version of a Published Work that appeared in final form in ACS applied materials and interfaces, copyright © American Chemical Society after peer review and technical editing by the publisher. To access the final edited and published work see <http://pubs.acs.org/doi/abs/10.1021/acsami.7b05012>. 1869-1876.

- [23] Pastorino, D.; Canal, C.; Ginebra, M.-P. Drug Delivery from Injectable Calcium Phosphate Foams by Tailoring the Macroporosity-Drug Interaction. *Acta Biomater.* **2015**, *12*, 250-259.
- [24] Kai, D.; Prabhakaran, M. P.; Chan, B. Q. Y.; Liow, S. S.; Ramakrishna, S.; Xu, F.; Loh, X. J. Elastic Poly(Epsilon-Caprolactone)-Polydimethylsiloxane Copolymer Fibers with Shape Memory Effect for Bone Tissue Engineering. *Biomed. Mater.* **2016**, *11*, 015007.
- [25] Felfel, R. M.; Poczka, L.; Gimeno-Fabra, M.; Milde, T.; Hildebrand, G.; Ahmed, I.; Scotchford, C.; Sottile, V.; Grant, D. M.; Liefelth, K. In Vitro Degradation and Mechanical Properties of Pla-Pcl Copolymer Unit Cell Scaffolds Generated by Two-Photon Polymerization. *Biomed. Mater.* **2016**, *11*, 015011.
- [26] Liao, G.; Jiang, S.; Xu, X.; Ke, Y. Electrospun Aligned Plla/Pcl/Ha Composite Fibrous Membranes and Their in Vitro Degradation Behaviors. *Mater. Lett.* **2012**, *82*, 159-162.
- [27] Guarino, V.; Causa, F.; Taddei, P.; di Foggia, M.; Ciapetti, G.; Martini, D.; Fagnano, C.; Baldini, N.; Ambrosio, L. Polylactic Acid Fibre-Reinforced Polycaprolactone Scaffolds for Bone Tissue Engineering. *Biomaterials* **2008**, *27*, 3662-3670.
- [28] Yu, S.; Tan, H.; Wang, J.; Liu, X.; Zhou, K. High Porosity Supermacroporous Polystyrene Materials with Excellent Oil-Water Separation and Gas Permeability Properties. *ACS Appl. Mater. Interfaces* **2015**, *12*, 6745-6753.
- [29] Yi, W.; Wu, H.; Wang, H.; Du, Q. Interconnectivity of Macroporous Hydrogels Prepared Via Graphene Oxide-Stabilized Pickering High Internal Phase Emulsions. *Langmuir* **2016**, *4*, 982-990.
- [30] Kim, Y. B.; Lee, H.; Kim, G. H. Strategy to Achieve Highly Porous/Biocompatible Macroscale Cell Blocks, Using a Collagen/Genipin-Bioink and an Optimal 3d Printing Process.

This document is the Accepted Manuscript version of a Published Work that appeared in final form in ACS applied materials and interfaces, copyright © American Chemical Society after peer review and technical editing by the publisher. To access the final edited and published work see <http://pubs.acs.org/doi/abs/10.1021/acsami.7b05012>. *ACS Appl. Mater. Interfaces* **2016**, *47*, 32230-32240.

[31] Hu, Y.; Gao, H.; Du, Z.; Liu, Y.; Yang, Y.; Wang, C. Pickering High Internal Phase Emulsion-Based Hydroxyapatite-Poly(Epsilon-Caprolactone) Nanocomposite Scaffolds. *J. Mater. Chem. B* **2015**, *18*, 3848-3857.

[32] Zhao, J.; Swartz, L. A.; Lin, W.-f.; Schlenoff, P. S.; Frommer, J.; Schlenoff, J. B.; Liu, G.-Y. Three-Dimensional Nanoprinting Via Scanning Probe Lithography-Delivered Layer-by-Layer Deposition. *ACS Nano* **2016**, *6*, 5656-5662.

[33] Ma, H.; Jiang, C.; Zhai, D.; Luo, Y.; Chen, Y.; Lv, F.; Yi, Z.; Deng, Y.; Wang, J.; Chang, J.; Wu, C. A Bifunctional Biomaterial with Photothermal Effect for Tumor Therapy and Bone Regeneration. *Adv. Funct. Mater.* **2016**, *8*, 1197-1208.

[34] Lin, K.-F.; He, S.; Song, Y.; Wang, C.-M.; Gao, Y.; Li, J.-Q.; Tang, P.; Wang, Z.; Bi, L.; Pei, G.-X. Low-Temperature Additive Manufacturing of Biomimetic Three-Dimensional Hydroxyapatite/Collagen Scaffolds for Bone Regeneration. *ACS Appl. Mater. Interfaces* **2016**, *11*, 6905-6916.

[35] Kim, Y. B.; Lee, H.; Kim, G. H. Strategy to Achieve Highly Porous/Biocompatible Macroscale Cell Blocks, Using a Collagen/Genipin-Bioink and an Optimal 3d Printing Process. *ACS Appl. Mater. Interfaces* **2016**, *47*, 32230-32240.

[36] Colver, P. J.; Bon, S. A. F. Cellular Polymer Monoliths Made Via Pickering High Internal Phase Emulsions. *Chem. Mater.* **2007**, *7*, 1537-1539.

[37] Li, Z.; Ngai, T. Macroporous Polymer from Core-Shell Particle-Stabilized Pickering Emulsions. *Langmuir* **2010**, *20*, 16186-16186.

[38] Zou, S.; Wei, Z.; Hu, Y.; Deng, Y.; Tong, Z.; Wang, C. Macroporous Antibacterial Hydrogels with Tunable Pore Structures Fabricated by Using Pickering High Internal Phase

This document is the Accepted Manuscript version of a Published Work that appeared in final form in ACS applied materials and interfaces, copyright © American Chemical Society after peer review and technical editing by the publisher. To access the final edited and published work see <http://pubs.acs.org/doi/abs/10.1021/acsami.7b05012>. Emulsions as Templates. *Polym. Chem.* **2014**, *14*, 4227-4234.

[39] Liu, H.; Wang, C. Chitosan Scaffolds for Recyclable Adsorption of Cu(I) Ions. *RSC Adv.* **2014**, *8*, 3864-3872.

[40] Muth, J. T.; Dixon, P. G.; Woish, L.; Gibson, L. J. Lewis, J. A. Architected Cellular Ceramics with Tailored Stiffness Via Direct Foam Writing. *P. Natl. Acad. Sci. USA.* **2017**, *8*, 1832-1837.

[41] Minas, C.; Carnelli, D.; Tervoort, E. Studart, A. R. 3d Printing of Emulsions and Foams into Hierarchical Porous Ceramics. *Adv. Mater.* **2016**, *45*, 9993-9999.

[42] Hu, Y.; Yang, Y.; Hu, M.; Gu, X.; Wang, C. Nanocomposite Porous Scaffolds for Bone Tissue Engineering by Emulsion Templating. *J. Control. Release* **2015**, *213*, E127.

[43] Hu, Y.; Gu, X.; Yang, Y.; Huang, J.; Hu, M.; Chen, W.; Tong, Z.; Wang, C. Facile Fabrication of Poly(L-Lactic Acid)-Grafted Hydroxyapatite/Poly(Lactic-Co-Glycolic Acid) Scaffolds by Pickering High Internal Phase Emulsion Templates. *ACS Appl. Mater. Interfaces* **2014**, *19*, 17166-17175.

[44] Vilchez, A.; Rodriguez-Abreu, C.; Esquena, J.; Menner, A. Bismarck, A. Macroporous Polymers Obtained in Highly Concentrated Emulsions Stabilized Solely with Magnetic Nanoparticles. *Langmuir* **2011**, *21*, 13342-13352.

[45] Ikem, V. O.; Menner, A. Bismarck, A. Tailoring the Mechanical Performance of Highly Permeable Macroporous Polymers Synthesized Via Pickering Emulsion Templating. *Soft Matter* **2011**, *14*, 6571-6577.

[46] Liu, X.; Okada, M.; Maeda, H.; Fujii, S.; Furuzono, T. Hydroxyapatite/Biodegradable Poly(L-Lactide-Co-Epsilon-Caprolactone) Composite Microparticles as Injectable Scaffolds by a Pickering Emulsion Route. *Acta Biomater.* **2011**, *2*, 821-828.

This document is the Accepted Manuscript version of a Published Work that appeared in final form in ACS applied materials and interfaces, copyright © American Chemical Society after peer review and technical editing by the publisher. To access the final edited and published work see <http://pubs.acs.org/doi/abs/10.1021/acsami.7b05012>.

[47] Zhang, G.; Wang, C. Pickering Emulsion-Based Marbles for Cellular Capsules. *Materials* **2016**, *7*, No. 572.

[48] Wei, Z.; Wang, C.; Liu, H.; Zou, S.; Tong, Z. Facile Fabrication of Biocompatible Plga Drug-Carrying Microspheres by O/W Pickering Emulsions. *Colloids Surf. B* **2012**, *91*, 97-105.

[49] Sugita, N.; Nomura, S.; Kawaguchi, M. Rheological and Interfacial Properties of Silicone Oil Emulsions Prepared by Polymer Pre-Adsorbed onto Silica Particles. *Colloids Surf. A* **2008**, *1-3*, 114-122.

[50] Sommer, M. R.; Alison, L.; Minas, C.; Tervoort, E.; Ruhs, P. A. Studart, A. R. 3D Printing of Concentrated Emulsions into Multiphase Biocompatible Soft Materials. *Soft Matter* **2017**, *9*, 1794-1803.

This document is the Accepted Manuscript version of a Published Work that appeared in final form in ACS applied materials and interfaces, copyright © American Chemical Society after peer review and technical editing by the publisher. To access the final edited and published work see <http://pubs.acs.org/doi/abs/10.1021/acsami.7b05012>.
Graphical Abstract

